A MODEL OF AN ECHO SOUNDER FOR FISH ABUNDANCE MEASUREMENTS

by: J.W.R. Griffiths and J.P. Smith
Electronic and Electrical Engineering Department,
University of Technology,
LOUGHBOROUGH, Leicestershire.

Introduction

In recent years there has been an increasing interest in acoustic techniques for the estimation of fish abundance. The literature, some of which is listed at the end of this paper, gives evidence of this. It is clear that there is a need for improved accuracy of the methods. The problem may be divided into two main areas:-

1. The reliability of the acoustic measurements in the estimation of bio-mass
2. The difficulty in obtaining reliable division of the estimated bio-mass into the abundance of the species of interest.

This report concentrates on the first of these problems and describes an attempt to establish a computer model of an echo sounder. The use of the computer model is, of course, like a mathematical model - limited by the accuracy with which the model represents the practical system. Several authors - in particular Ehrenburg - have developed mathematical models and used these to determine the accuracy of estimation of bio-mass. However, it is the authors' contention that much of the physical understanding is lost in a mathematical model and that the computer model offers a better approach, allowing interaction between the user and the model.

The Model

Referring to Fig. 1 let the acoustic pulse transmitted in the direction of the acoustic axis be $x(t) \cos \omega t$, $x(t)$ being the pulse envelope shape and ω the carrier frequency.

The signal reaching the target will be delayed in time due to the finite acoustic velocity and in addition its amplitude will be dependent on

(a) the angular position of the target relative to the acoustic axis

(b) on square law spreading, and

(c) the attenuation of the acoustic wave in the medium.

A proportion of this incident signal will be re-radiated by the target and the strength (and phase) of the re-radiated wave will depend on the size, shape and construction of the target. This wave will then be subject to the same losses and delay on the return path as on the forward path.

Thus the signal received from a single point target at a position R_i, θ_i, ϕ_i relative to the transmitter can be represented by the following expression

$$v_i = A_i \, \beta(\theta_i, \phi_i) \, x(t - \frac{2R_i}{c}) \cos \omega(t - \frac{2R_i}{c}) \quad \ldots\ldots\ldots\ldots\ldots\ldots (1)$$

A_i is a factor which will depend on the square law spreading loss, the attenuation of the medium, the sensitivity of the receiver and the target strength. $\beta(\theta_i, \phi_i)$ takes into account the directivity both on transmission and reception.

It is convenient to use range (depth) rather than time as the variable, as this is how the signal is normally displayed in echo-sounders.

Putting $R = \frac{ct}{2}$ we get

$$v_i = A_i \, \beta(\theta_i, \phi_i) \, x\{\frac{2}{c}(R-R_i)\} \cos \frac{2\omega}{c}(R-R_i) \quad \ldots\ldots\ldots\ldots\ldots\ldots (2)$$

Equation (2) can be expressed as the convolution of two functions

$$h(R) = x(\frac{2R}{c}) \cos(\frac{2\omega R}{c})$$

and $A_i \beta(\theta_i, \phi_i) \delta(R - R_i)$

$= T_i \delta(R-R_i)$

Thus $v_i = h(R) * T_i \delta(R-R_i)$ ..... (3)

When we consider a number of targets

$v = \sum_i v_i = h(R) * \Sigma T_i \delta(R-R_i)$ ..... (4)

Thus we can represent the behaviour of the echo sounder system as a linear system having an impulse response h(R) and fed with a series of impulses of strength T_i occurring at ranges R_i as shown in Fig. 2.

A digital computer does not deal with continuous functions and hence we need to divide the range up into a large number of small intervals each of δ units. In displaying the output however we can linearly interpolate between the samples to obtain a continuous display.

Arbitrarily we normalise the unit of range such that in the above expressions $\frac{2}{c} = 1$, and in addition we choose the angular frequency such that in these units $\omega = 1$. These decisions affect only the range scale of the final output.

In Fig. 3a we see a photograph of the output of the computer for a single point target for a particular set of conditions. The pulse shape used in terms of the normalised range units was $x(R) = \frac{1}{2}(1 - \cos \frac{2\pi R}{\Delta})$ and the carrier frequency ω is unity.

This is a typical received sonar waveform from a single target but of course can be changed at will in the program if required.

A perfect envelope detector would plot the modulus of this waveform which is seen in Fig. 3b.

Any appropriate curve can be fed into the computer for the angular

sensitivity $\beta(\theta, \phi)$. However, it was convenient to use a Gaussian shape for the initial trials since in addition to being easily generated and mathematically simple, it represents a fairly close approximation to the practical situation. Hence it was assumed that

$$\beta(\theta,\phi) = e^{-\theta^2} e^{-\phi^2}$$

Generation of a suitable target distribution

We imagine the space with which we are concerned to be divided by a set of spherical shells centred on the location of the echo sounder and spaced by the range increment δ.

We use a Poisson distribution to determine on a random basis which of these shells contain a target assuming that δ is small enough so that there is not more than one target in each interval. The average value of the Poisson distribution determines the average number of targets and hence the target density in range. Two points should be noted here.

(1) It would be quite easy to extend the analysis to have more than one target per range interval.

(2) The targets are assumed to be point sources at this stage. Later the simulation will be developed to take into account the various properties of the target other than its 'target strength', e.g. length, directivity, etc.

Having decided that there is a target at a particular range R_i we choose at random a value for θ_i and ϕ_i from a uniform distribution extending between given angular limits which could if required be $\pm\pi$. However, if we are dealing with relative narrow beamwidths it is not necessary to extend the angular range much beyond the beamwidth. Increase of the angular range for a given beam pattern $\beta(\theta,\phi)$ obviously reduces the average target strength which, of course, ties up with the fact that the volume target density is reduced (See Appendix 1).

The amplitudes A_i are range dependent as well as being dependent on the target strengths but in practice by the use of T.V.G. in the receiver, this range dependence can be compensated. A_i can then be given a suitable distribution, e.g. Gaussian and it is convenient to normalise the mean to unity.

Any typical trace can be displayed on the C.R.T. output from the computer, and an example is shown in Fig. 4.

Estimation of target number

In Appendix 2 it is shown that the energy of the pulse envelope for the particular pulse shape chosen is $\frac{3\Delta}{8\delta}$.

We have standardized the target strength A_i as having a mean of unity and in Appendix 1 we have determined the mean square value for $\beta(\theta,\phi)$ as

$$\frac{\pi}{8\theta_1\phi_1} \operatorname{erf}(\sqrt{2}\theta_1) \operatorname{erf}(\sqrt{2}\phi_1)$$

From this information it is thus possible to calculate the expected average energy of a single pulse.

By dividing the measured energy from the particular trace by this quantity we can then estimate the number of targets. The program is designed to carry out this calculation and the result may then be compared with the actual number of targets which is, of course, known.

The program is arranged to go through this procedure a number of times so that a set of results are obtained. These results can be plotted by the computer in the form of a graph representing a plot of the estimated number of targets against the actual target number, and in addition the computer can calculate and plot the best fitting straight line to the results. This line should, of course, have a slope of unity and pass through the origin.

Discussion of Results

Some typical results are shown in Fig.5 and Fig.6. The values of θ_1 and ϕ_1 were chosen as 1.5 since this takes into account any target of reasonable size within the beam of the system (see Appendix 1).

A plot of the slopes for a number of cases showed that the model exhibits some anomaly for very closely spaced targets. It is probable, however, that this is an artifice of the particular example chosen. When the average target spacing is 3 units this is equivalent to about half a wavelength of the acoustic pulse. Thus there will be a tendency for adjacent pulses to cancel out and so decrease the measured energy. This is, of course, a real effect and should targets be as close as this the same result could occur.

For most of the results the measurement of energy provided a reasonable estimate of the number of targets provided sufficient results are averaged. However, the large variance of the results shows clearly that on any individual trace the measurement of energy could give a very misleading result.

The results so far show that the model is very promising but requires some further validation before too much weight is put on these conclusions. Further the model requires to be extended to approach more nearly the practical situation.

Acknowledgement

The authors would like to acknowledge financial support from the Ministry of Agriculture, Food and Fisheries, Lowestoft.

Appendix 1

Mean Square of Directional Pattern

If the direction pattern is $\beta(\theta,\phi)$ then the mean square is given by

$$\overline{\beta^2(\theta,\phi)} = \int\int \beta^2(\theta,\phi)\ \rho(\theta,\phi)\ d\theta d\phi$$

where $\rho(\theta,\phi)$ is the joint probability density for θ & ϕ.
Since θ and ϕ are chosen independently and are uniformally distributed over the ranges $\pm\ \theta_1$ and $\pm\phi_1$ respectively then

$$\rho(\theta,\phi) = \rho(\theta).\ \rho(\phi) = \frac{1}{2\theta_1} \cdot \frac{1}{2\phi_1} \qquad \begin{matrix} -\theta_1 < \theta < \theta_1 \\ -\phi_1 < \phi < \phi_1 \end{matrix}$$

$$= 0 \quad \text{elsewhere}$$

$$\therefore\ \overline{\beta^2(\theta,\phi)} = \frac{1}{4\theta_1\phi_1} \int_{-\theta_1}^{\theta_1}\int_{-\phi_1}^{\phi} \beta^2(\theta,\phi)\ d\theta d\phi$$

we have assumed in the text that

$$\beta(\theta,\phi) = e^{-\theta^2}\ e^{-\phi^2} = \beta_1(\theta).\ \beta_1(\phi)$$

Thus the double integral is separable into two single integrations viz:

$$\overline{\beta^2(\theta,\phi)} = \frac{1}{2\theta_1}\int_{-\theta_1}^{\theta_1} e^{-2\theta^2}\ d\theta \cdot \frac{1}{2\phi_1}\int_{-\phi_1}^{\phi_1} e^{-2\phi^2}\ d\phi$$

$$\frac{1}{2\theta_1}\int_{-\theta_1}^{\theta_1} e^{-2\theta^2}\ d\theta = \frac{1}{\theta_1}\int_{0}^{\theta_1} e^{-2\theta^2}\ d\theta$$

$$= \frac{1}{\sqrt{2}\theta_1}\int_{0}^{\sqrt{2}\theta_1} e^{-x^2}\ dx \quad \text{where } x = \sqrt{2}\theta$$

$$= \frac{\sqrt{\pi}}{2\sqrt{2}\theta_1}\ \text{erf}\ (\sqrt{2}\theta_1)$$

similarly $\frac{1}{2\phi_1}\int_{-\phi_1}^{\phi_1} e^{-2\phi^2}\,d\theta = \frac{\sqrt{\pi}}{2\sqrt{2}\phi_1}\ \mathrm{erf}(\sqrt{2}\phi_1)$

$$\therefore\ \overline{\beta^2(\theta,\phi)} = \frac{\pi}{8\theta_1\phi_1}\ \mathrm{erf}(\sqrt{2}\theta_1)\ \mathrm{erf}(\sqrt{2}\phi_1)$$

$$= \frac{\pi}{8\theta_1^2}\ \mathrm{erf}^2(\sqrt{2}\theta_1) \quad \text{if} \quad \theta_1 = \phi_1$$

For large values of θ_1 $\mathrm{erf}(\sqrt{2}\theta_1) \to 1$

$$\therefore\ \overline{\beta^2(\theta,\phi)} \to \frac{\pi}{8\theta_1^2}$$

e.g. it will be seen that for $\theta_1 = 2$ this expression gives the value 0.09818 whereas the exact value is 0.09816.

Table 2

θ_1	$\overline{\beta^2(\theta,\phi)}$
0.5	0.73195
1.0	0.35775
1.5	0.17354
2.0	0.09816

Appendix 2

Integrated Mean Square of pulse envelope (pulse energy)

$$= \overline{|x(R)|^2}$$

$$= \int_0^{\Delta} \tfrac{1}{4}(1 - \cos \frac{2\pi R}{\Delta})^2 \, dR$$

if the pulse was a continuous function of range

$$= \tfrac{1}{4} \int \{1 - 2 \cos \frac{2\pi R}{\Delta} + \cos^2 \frac{2\pi R}{\Delta} \} \, dR$$

$$= \tfrac{1}{4} \int_0^{\Delta} \{1 - 2 \cos \frac{2\pi R}{\Delta} + \tfrac{1}{2} + \tfrac{1}{2}\cos \frac{4\pi R}{\Delta} \} \, dR$$

$$= \frac{3\Delta}{8}$$

In the computer model the calculation will be carried out using a summation rather than integration as $R = n\delta$, δ being the range increment.

Let $\Delta = N\delta$

$$\therefore \quad \overline{|x(R)|^2} = \sum_{n=0}^{N} \tfrac{1}{4}(1 - \cos \frac{2\pi n\delta}{N\delta})^2$$

$$= \sum_{n=0}^{N} \tfrac{1}{4}(1 - \cos \frac{2\pi n}{N})^2$$

$$= \tfrac{1}{4} \sum_{n=0}^{N} (1 - 2 \cos \frac{2\pi n}{N} + \tfrac{1}{2} + \tfrac{1}{2} \cos \frac{4\pi n}{N})$$

for $n = 0$ this expression is zero.

$$\therefore \quad \overline{|x(R)|^2} = \frac{3N}{8} + \sum_{n=1}^{N} (2 \cos \frac{2\pi n}{N} + \tfrac{1}{2} \cos \frac{4\pi n}{N})$$

$$= \frac{3N}{8} = \frac{3\Delta}{8\delta}$$

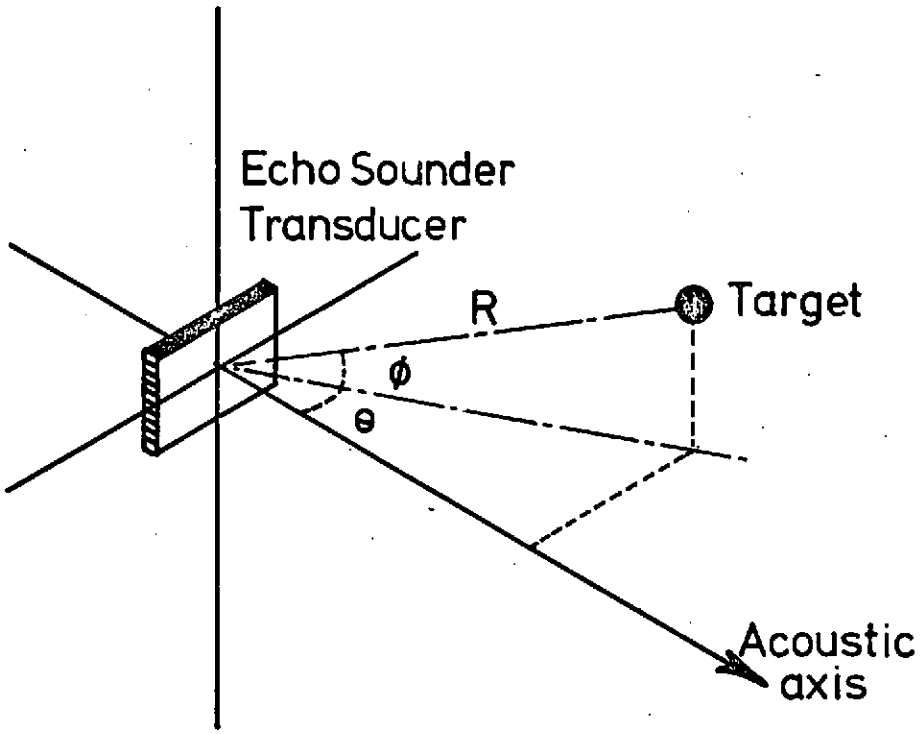

Fig. 1. Showing the axes of measurement.

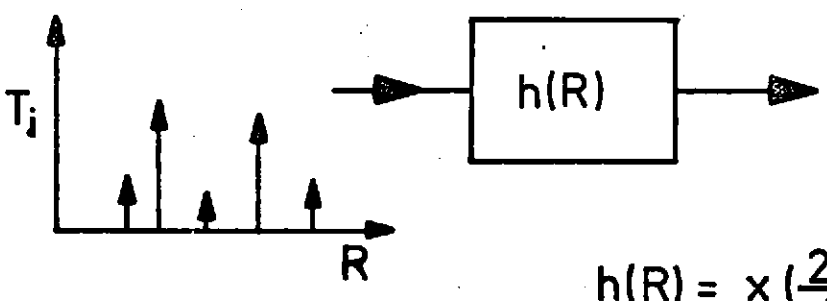

$$h(R) = x\left(\frac{2R}{C}\right) \cos\left(\frac{2\omega R}{C}\right)$$

Fig. 2. Representation as Linear System

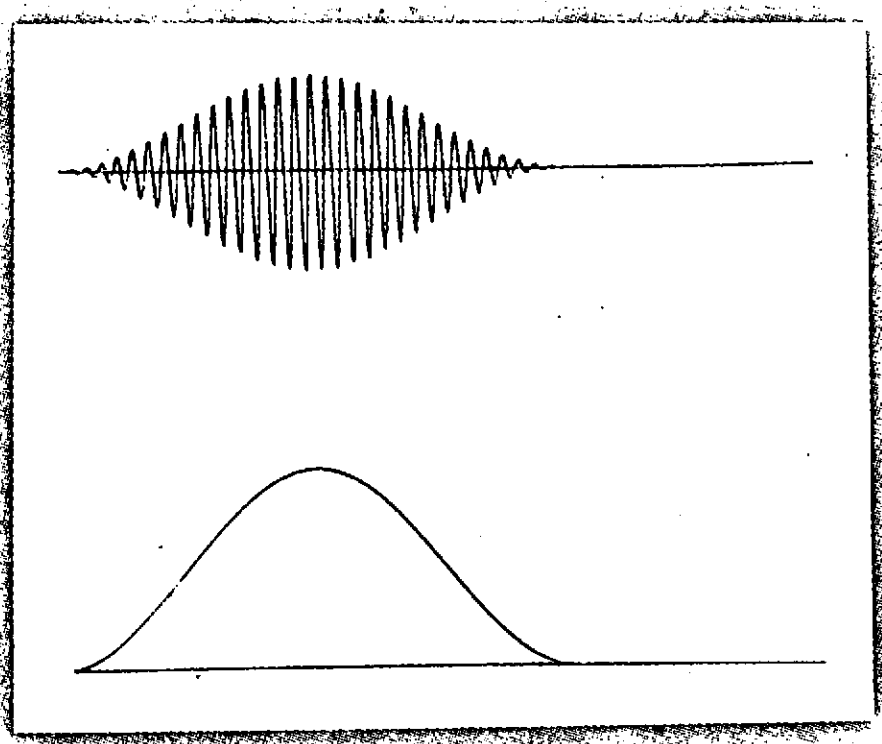

Fig. 3. Single target output

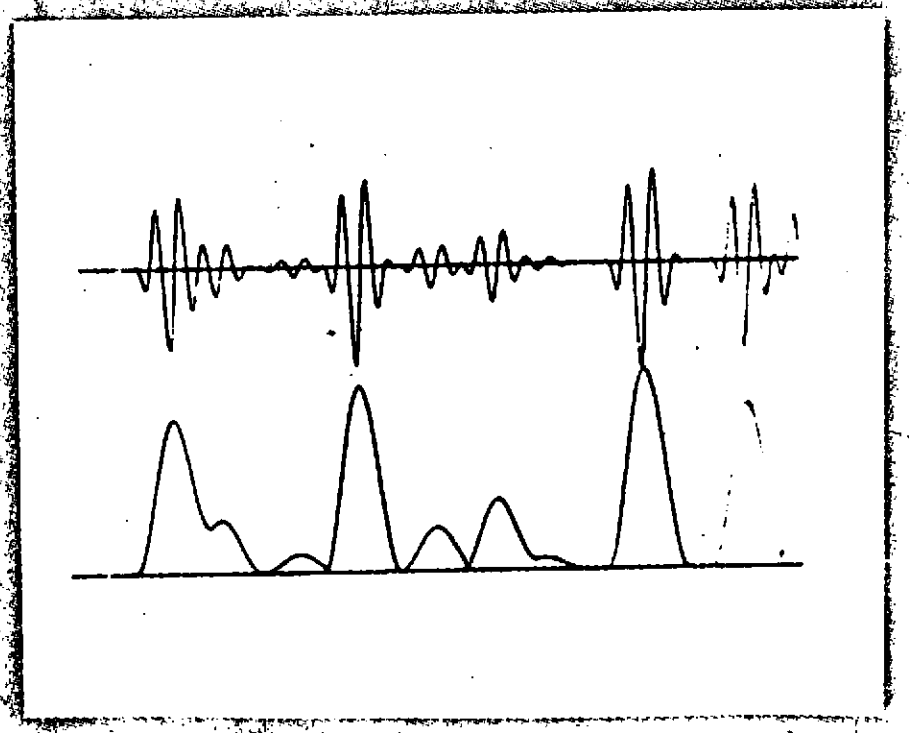

Fig. 4. Multiple target output

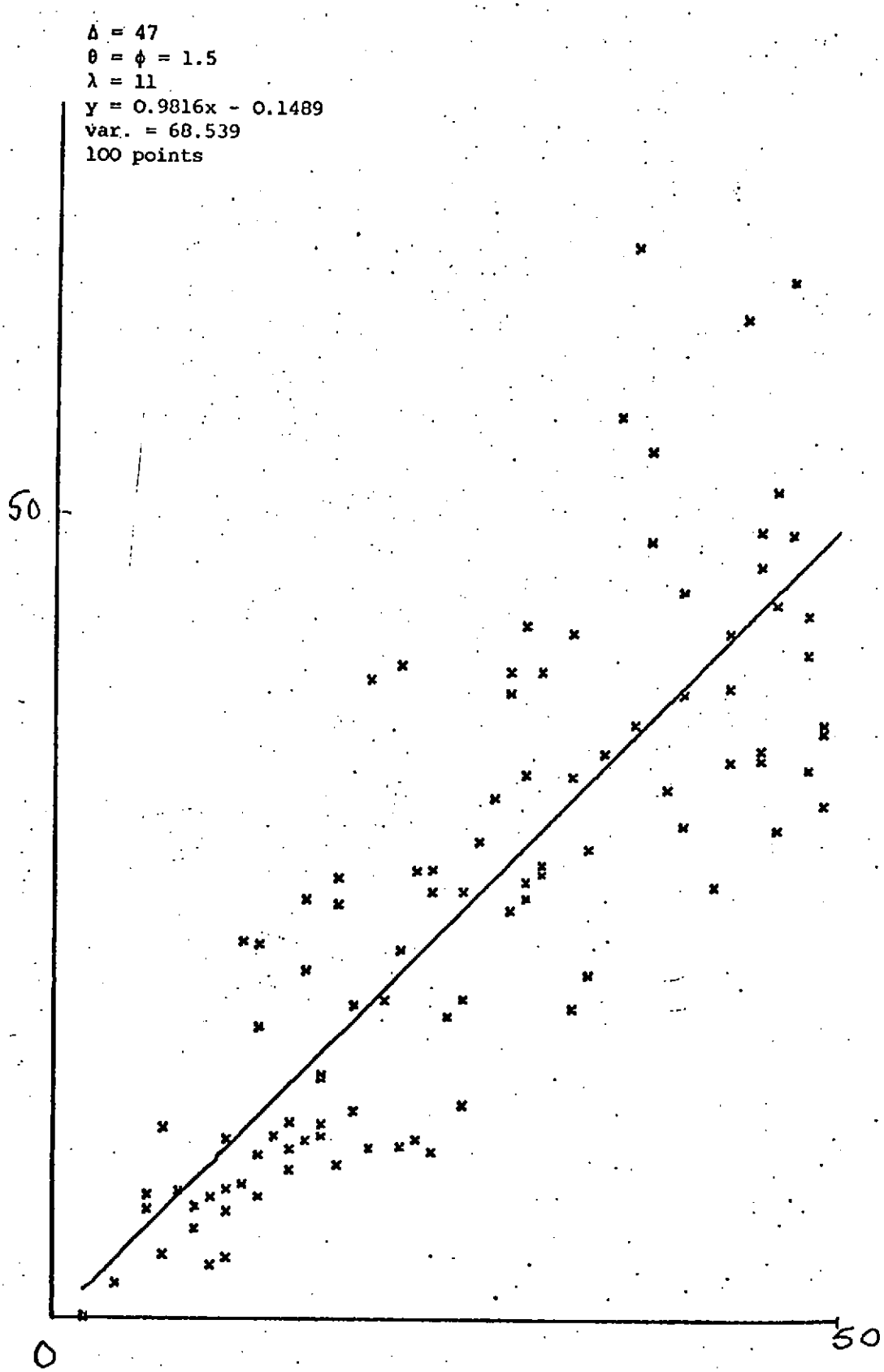

Figure 5

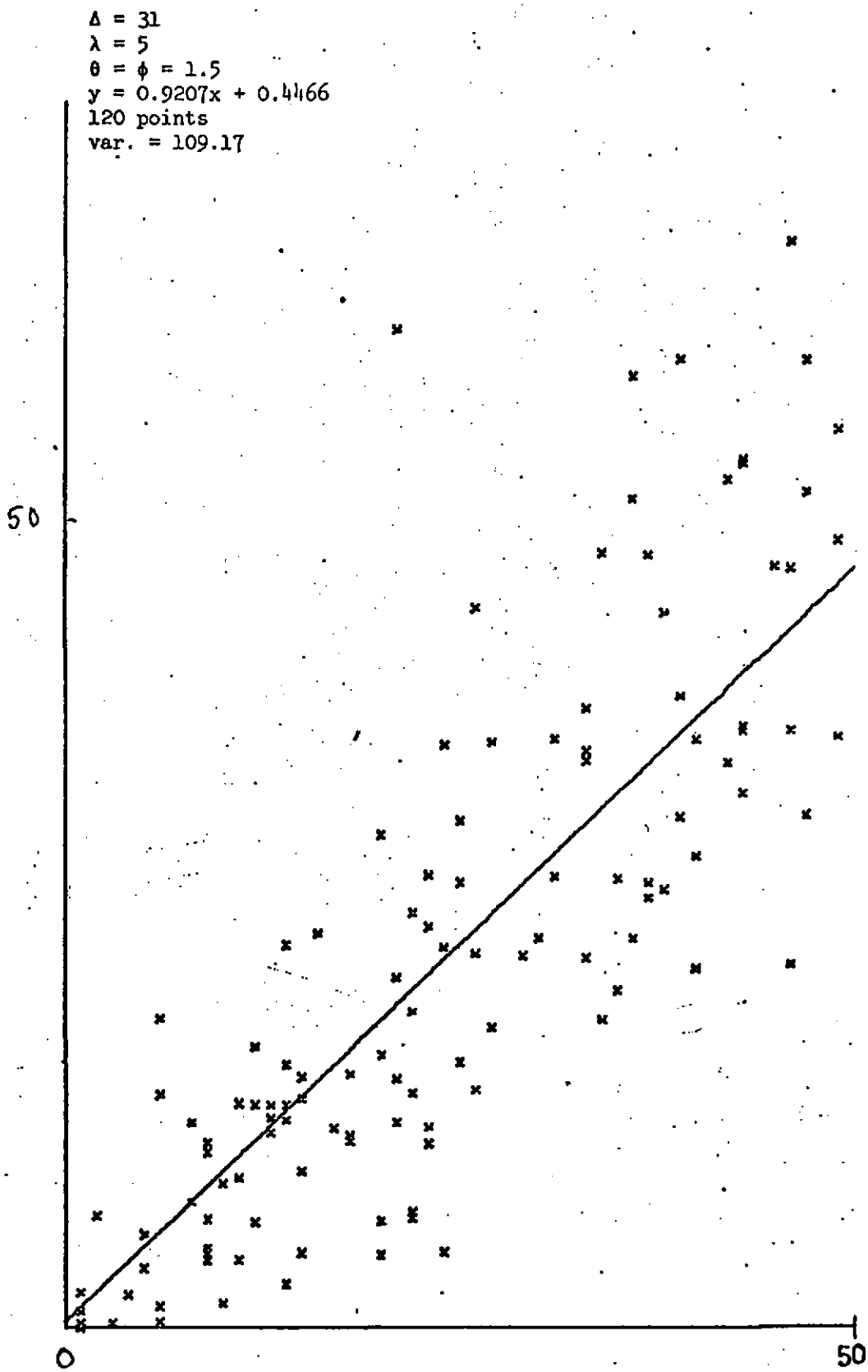

Figure 6